UNIVERSITY OF BIRMINGHAM

Indentation Plastometry of Particulate Metal Matrix Composites, Highlighting Effects of Microstructural Scale

Reiff-Musgrove, Rebecca; Gaiser-Porter, Marcus; Gu, Wenchen; Campbell, Jimmy E.; Lewis, Peter; Frehn, Andreas; Tarrant, Andrew D.; Tang, Yuanbo T.; Burley, Max; Clyne, Trevor William

Link to publication on Research at Birmingham portal

Indentation Plastometry of Particulate Metal Matrix Composites, Highlighting Effects of Microstructural Scale

*Rebecca Reiff-Musgrove, Marcus Gaiser-Porter, Wenchen Gu, Jimmy E. Campbell, Peter Lewis, Andreas Frehn, Andrew D. Tarrant, Yuanbo T. Tang, Max Burley, and Trevor William Clyne**

Herein, it is concerned with the use of profilometry-based indentation plastometry (PIP) to obtain mechanical property information for particulate metal matrix composites (MMCs). This type of test, together with conventional uniaxial testing, has been applied to four different MMCs (produced with various particulate contents and processing conditions). It is shown that reliable stress–strain curves can be obtained using PIP, although the possibility of premature (prenecking) fracture should be noted. Close attention is paid to scale effects. As a consequence of variations in local spatial distributions of particulate, the "representative volume" of these materials can be relatively large. This can lead to a certain amount of scatter in PIP profiles and it is advisable to carry out a number of repeat PIP tests in order to obtain macroscopic properties. Nevertheless, it is shown that PIP testing can reliably detect the relatively minor (macroscopic) anisotropy exhibited by forged materials of this type.

1. Introduction

Interest in particulate-reinforced metal matrix composites (MMCs) became strong in the 1980s, and they have been in significant commercial use for over 20 years. The particles are

R. Reiff-Musgrove, W. Gu, J. E. Campbell, M. Burley, T. W. Clyne
Plastometrex Ltd.
204 Science Park, Milton Road, Cambridge CB4 0GZ, UK
E-mail: twc10@cam.ac.uk

M. Gaiser-Porter, T. W. Clyne
Department of Materials Science
27 Charles Babbage Road, Cambridge CB3 0FS, UK

P. Lewis, A. D. Tarrant
Materion Ltd.
1 RAE Road, Farnborough, Hampshire GU14 6XE, UK

A. Frehn
Materion Brush GmbH
Motorstraße 34, 70499 Stuttgart, Germany

Y. T. Tang
Department of Materials
Parks Road, Oxford OX2 3PH, UK

The ORCID identification number(s) for the author(s) of this article can be found under https://doi.org/10.1002/adem.202201479.

normally ceramic, with SiC and Al_2O_3 being the most common. A range of metallic matrices have been used, but aluminum alloys of various types are among the most popular. The addition of such reinforcement offers potential for substantial enhancements in the stiffness and strength (resistance to plastic deformation) of the matrix,[1–4] while retaining acceptable levels of toughness. Such materials are also attractive in terms of tribological characteristics, commonly exhibiting major improvements in resistance to various types of wear.[5,6] For such enhancements to be significant, reinforcement contents are needed of at least about 10% (by volume) and levels of 20% or 30% are commonly employed. Commercial usage of composite materials of this type has extended to a range of applications, including several in the aerospace industry.

It has always been clear, however, that the processing conditions, and hence the details of the microstructure, are of critical importance if optimum properties are to be obtained. While several types of processing route have been employed to produce various MMCs, powder blending and consolidation has in general been the most successful one for particulate MMCs. In this case, process optimization is usually aimed at producing a uniform spatial distribution of relatively fine particles that are well bonded to the matrix, with little or no porosity. A number of studies[7–9] have been aimed at clarifying the effects involved, including those concerning powder size, blending techniques, sintering, and consolidation conditions, etc. There have also been studies[10,11] in which an inverse correlation has been established between the degree of clustering (i.e., the level of inhomogeneity of particle distribution) and the ductility. In contrast, it may be noted that some effects, such as the creation of anisotropy from alignment of "stringers" of reinforcement particles, could be beneficial and should in any event be monitored and controlled. Moreover, the microstructure of the matrix is likely to be affected by the presence of particulate, so modifications to thermomechanical treatments may be needed for optimization of age hardening and other characteristics. For example, previous work[12,13] has shown that recrystallization characteristics can be sensitive to the level and type of reinforcement.

Another issue of potential significance for particulate MMCs is the presence of internal residual stresses, largely arising

from differential thermal contraction during the latter stages of production. These have been studied in some depth.[14–18] They certainly have the potential to be significant, since a typical difference in thermal expansivity between particle and matrix is about 20 microstrain K^{-1}, so that a temperature drop of, say, 500 K will generate a (large) misfit strain of about 10 millistrain. In fact, since the resulting stresses are, on average, purely hydrostatic (compressive in the particles and tensile in the matrix), they tend to have less effect on the behavior than for MMCs that incorporate directionality, such as aligned fiber composites. Residual stresses in those have nonzero (average) deviatoric components and those in the matrix can have pronounced effects on plasticity (and creep) characteristics of the composite. Nevertheless, it should be noted that relatively large residual stresses are in general present in particulate MMCs. Moreover, on a local scale, there are nonzero deviatoric components—for example, tensile hoop stresses are present in the matrix immediately adjacent to a (spherical) particle. These local stresses have the potential to affect the way that plasticity develops under macroscopic loading. In particular, it has repeatedly been suggested,[14–17] from both modeling and experimental work, that one effect of these local residual stresses is to make the macroscopic yielding more progressive (transient), so that the yield point is less well defined. This certainly tends to be a feature of many experimental tensile stressstrain –curves of particulate MMCs.

One consequence of the sensitivity of microstructure and properties to the processing conditions, including the level and nature of the reinforcement, is a pressing need for a quick and convenient method of characterising the mechanical properties, including any variations with location in the sample and any anisotropy that may have arisen. There is therefore interest in applying the recently-developed methodology of profilometry-based indentation plastometry (PIP) to composite materials of this type. This procedure is based on iterative FEM simulation of the indentation process, with the plasticity parameters (in a constitutive law) being repeatedly changed until optimal agreement is reached between experimental and predicted outcomes. This is done by converging in parameter space on the set of values for which the misfit between modeled and measured profiles, characterized via a sum of squares parameter, is a minimum. There are several constitutive laws that could be used to capture the plasticity characteristics, but the one used in the current work is that of V_{oce}

$$\sigma = \sigma_s - (\sigma_s - \sigma_Y)e^{-\varepsilon/\varepsilon_0} \qquad (1)$$

in which σ_Y is the yield stress, σ_s is a "saturation" level, and ε_0 is a characteristic strain for the exponential approach of the stress toward this level. It should be noted that the elastic constants of the material (Young's modulus and Poisson ratio) are required as input parameters for the modeling. However, the outcome does not have a high sensitivity to these values, which need only be specified to an accuracy of about 10–15%. Simply knowing the base metal is usually sufficient for this.

While the target outcome used in much early work on obtaining stress–strain curves from indentation data via inverse FEM modeling was the load–displacement plot, it has become clear that using the residual indent profile offers major advantages. These are explained in some detail in a recent review paper.[19]

In summary, these are (a) improved sensitivity of the experimental outcome to the stress–strain relationship, (b) a capability to detect the presence and sense of any (in-plane) anisotropy in the sample (via a lack of radial symmetry in the profile), (c) improved experimental convenience and accuracy, by eliminating the need to make any measurements during the test or to be concerned about the compliance of the loading train, and (d) potential for obtaining further information by carrying out indentation to more than one depth and measuring the profiles for them. Detailed information is also available[19] concerning the sources and likely magnitudes of errors that could arise in various ways. The superior reliability of PIP to the ("Instrumented Indentation Technique"—IIT) methodology of converting a load–displacement plot directly to a stress–strain curve via analytic relationships has been clearly demonstrated.[20] Integrated facilities are now available that allow stress–strain curves to be obtained from a single indentation experiment within a timescale of a couple of minutes or so.

Advantages of the PIP procedure, compared with uniaxial testing, include minimal specimen preparation requirements and a capability to map properties over a surface on a relatively fine (≈a mm) scale. These are also offered by hardness testing, but hardness numbers are not well-defined material properties and they should be regarded as no better than semi-quantitative guides to the plasticity of metals.[21] There are several types of sample for which the fine-scale mapping of material response, including anisotropic effects, is a very attractive prospect. A recent paper[22] covers its use for monitoring variations in stress–strain relationships in the vicinity of welds. Similar attractions apply to the testing of MMCs, for which both local property variations and the presence of anisotropy are of interest. The present work is therefore aimed at comparing the outcomes of PIP testing a range of particulate MMC materials with those from conventional testing, and also correlating these results with microstructural observations.

There have been a few studies[23,24] involving nanoindentation of MMCs, but such testing cannot generate bulk properties. In fact, while this is the case for most materials, partly because nanoindentation commonly takes place within single grains, it is particularly true of MMCs, since there is no possibility of deforming a representative volume during a test (with a typical lateral indent size of a few microns and a depth of no more than a micron). The PIP procedure involves deforming a region with dimensions of the order of hundreds of microns, and this volume is expected to be a sufficiently large to be representative for particulate MMCs, at least for cases in which the particles are relatively small (no larger than a few tens of microns) and homogeneously distributed.

Some previous indentation works on particulate MMCs have been undertaken with similarly large (spherical) indenters,[25,26] but these did not involve residual profile measurements or iterative FEM simulation and did not lead to successful extraction of stress–strain relationships from indentation data. There have also been a few purely theoretical studies,[27] but confirmation of the assumptions incorporated in such models is always problematic. One suggestion that has, however, been made[28] is that (large-scale) indentation may cause "crowding" of the particulate during the deformation and that this could affect the response. This possibility is worth investigating, since it has certainly not

**ADVANCED
SCIENCE NEWS**

www.advancedsciencenews.com

**ADVANCED
ENGINEERING
MATERIALS**

www.aem-journal.com

been confirmed so far. The current work constitutes the first reported application of PIP testing to MMCs, allowing comparison between indentation -inferred and uniaxially obtained stress–strain curves.

2. Experimental Section

2.1. Materials

Particle-reinforced MMC materials were produced at Materion, using powder blending and consolidation procedures. The matrix was in all cases 6063 Al alloy, with an average original powder particle size of about 70–100 μm. Two grades of SiC particulate were used, with the finer one having a size of up to about 0.7 μm and the coarser one up to about 3 μm. Four types of sample were produced, covering a range of combinations of reinforcement content and processing conditions—as listed in **Table 1**. All four of these materials were produced in the form of "slabs", which were approximately 15 mm thick (and with lateral dimensions of at least about 30 mm). No distinction could be drawn between the two "in-plane" directions, and it was expected that there would be no in-plane anisotropy. However, the through-thickness direction could be distinguished from the two in-plane directions. For the HIPed material, this direction would be expected to be equivalent to the other two, but for the forged materials (in which it was the direction in which the forging force was being applied), some differences might be expected.

2.2. Microstructural Examination

Optical microscopy was used mainly to obtain an indication of the spatial distribution on the reinforcement particles on various length scales. There is particular interest in how they are distributed on the scale of a few hundred microns up to an mm or so, since this is the order of magnitude of the linear dimensions of the region deformed during PIP testing. In fact, since the particle size is approximately either 0.7 or 3 μm, they cannot readily be resolved individually using optical microscopy. However, a clear impression can nevertheless be obtained concerning their overall spatial distribution. Samples were prepared by grinding and polishing to 3 μm finish and viewed using reflected light under bright-field conditions.

Microstructures were also examined at higher magnification, using scanning electron microscopy (SEM), after the same sample preparation procedures. A Zeiss Merlin field-emission gun scanning electron microscope (FEG-SEM) was used, with images being obtained in both back scattered and secondary electron modes, with an accelerating voltage of 15 kV. High-resolution electron backscattered diffraction (EBSD) maps were also acquired using a Bruker eFlash[HR] detector on the XZ-orientation. The same sample was further fine polished using a Gatan PIPS II precision ion polishing system (Model 695). Two Ar-ion guns were positioned at 8° to the sample surface at 8 keV for 16 min. The sample was rotated at 6 rpm in vacuum. EBSD maps were acquired using an accelerating voltage of 15 kV with a probe current of 20 nA. The Kikuchi diffraction patterns were stored at 320×240 resolution with a step size of 223 nm. ESPRIT 2.3 and HKL Channel 5 software were used for data processing.

2.3. Uniaxial Testing

Tensile tests were carried out in accordance with BS EN/ISO 6892-1:2009 and ASTM E8M, using an Instron 3369 loading frame with a 50 kN capacity. Cylindrical specimens were used, with a 5 mm diameter, 25 mm gauge length, and surface finish $\leq 0.4 R_a$. Prior to testing, samples were put through a precycle to remove slack from the loading train. Following this, the tests were completed at a constant strain rate of about 10^{-4} s^{-1}. Strain was measured to failure, via a clip-on dual averaging extensometer with a maximum strain limit of 10%. For samples that reached 10% strain without failure, the test was paused and restarted to reach eventual failure. Samples were tested only in "in-plane" directions.

Compression tests were also carried out using an Instron 3369 loading frame, with a 50 kN capacity. Samples were in the form of cylinders (4 mm diameter and 4 mm long). No lubricant was used. Displacement was measured using a linear variable displacement transducer (LVDT), attached to the upper platen and actuated against the lower one. In addition, Techni-Measure 1 mm linear strain gauges were attached to both sides of each sample. They have a range of up to about 2%. The average value from these two was used to apply a compliance correction to the LVDT data. This also removes the uncertainty associated with the "bedding down" effect. Compression testing was carried out in both "in-plane" and "through-thickness" directions.

2.4. Indentation Plastometry

Four steps are involved in obtaining a tensile (or compressive) nominal stress–strain curve from a PIP test. These are (a) pushing a hard indenter into the sample with a known force, (b) measuring the (radially symmetric) profile of the indent, (c) iterative FEM simulation of the test until the best-fit set of (V_{oce}) plasticity parameter values is obtained, and (d) converting the resultant (true) stress–strain relationship to a nominal stress–strain curve that would be obtained during uniaxial testing. For tensile testing, up to the onset of necking, this conversion can be done using the standard analytical relationships. For accurate conversion to a compressive nominal stress–strain relationship, or for a tensile one after the onset of necking, FEM simulation of the test is

Table 1. Sample designations and processing conditions. (CWQ = Cold Water Quench; PGQ = PolyGlycol Quench).

Designation	Alloy	Particle content	Process	Heat treatment
Fine-20-HIP	6063	20 vol% 0.7 μm SiC	HIP of billet	T6 CWQ
Fine-20-Forge	6063	20 vol% 0.7 μm SiC	HIP, followed by forging	T6 PGQ
Fine-30-Forge	6063	30 vol% 0.7 μm SiC	HIP, followed by forging	T6 PGQ
Coarse-30-Forge	6063	30 vol% 3 μm SiC	HIP, followed by forging	T6 PGQ

**ADVANCED
SCIENCE NEWS**

www.advancedsciencenews.com

**ADVANCED
ENGINEERING
MATERIALS**

www.aem-journal.com

required (with a friction coefficient required for a compression test). Full details are provided in a recent review paper.[19]

Indentation was carried out into both top (x–y) and transverse (x–z) surfaces. Penetration ratio (depth over indenter radius) values of around 15–20% were used. Most of the indentation was carried out using a sphere of 1 mm radius, with the indent profiles measured using a stylus profilometer. It became clear that, while some of the indents appeared to be radially symmetric, others exhibited a degree of asymmetry—i.e., variations in pile-up height with scan angle. This is commonly taken to be indicative of anisotropy in the material, with directions in which the pile-up is higher being "softer" than other directions. However, it became clear that what was being observed was more complex than being due to consistent anisotropy. For example, sometimes the two halves of a single scan were asymmetric. This is suggestive of inhomogeneity in the sample, on a relatively coarse scale (of the order of the indenter radius). Microstructural examinations (§3) confirmed that such variations are indeed present in these materials.

This was investigated further by more detailed study of the Fine-20-HIP material, in which no overall anisotropy is expected. A relatively large number of PIP tests were carried out, using four different ball sizes—with radii of 0.5, 1.0, 1.5, and 2.0 mm. The profilometry was in this case carried out using an optical interferometric system (NetGAGE3D from Isra Vision), facilitating the rapid examination of multiple scan directions. This work was aimed at exploring statistical aspects of the outcome—particularly related to the potential detection of local anisotropy or inhomogeneity (apparent as differences in pile-up height in different directions and locations).

3. Microstructure

3.1. Importance of Scale

To assist with interpretation of the mechanical testing outcomes, it is helpful with these materials to have a clear picture of their microstructures. This relates particularly to issues of scale. While conventional uniaxial testing involves interrogation of the material on a very coarse scale (of the order of several mm in linear dimensions), the region deformed during PIP testing is smaller—of the order of a few hundred μm to several hundred μm in linear dimensions. For most materials, such a region will be large enough to constitute a "representative" volume—for example, it will commonly contain "many" grains (capturing the effects of grain size and shape, texture, grain boundary structure, etc). However, in these MMCs, there is a possibility that the spatial distribution of the particulate could be such as to create inhomogeneity and/or anisotropy on a length scale of the order of hundreds of μm. If so, there could be point-to-point variations and/or apparent anisotropy (even if the material is macroscopically homogeneous and isotropic).

3.2. Scanning Electron Microscopy and Electron Backscattered Diffraction Microscopy

The SEM is potentially helpful for studying the size and shape of individual particles, as well as their spatial distribution on a local scale. For example, **Figure 1** shows the microstructure of the Coarse-30-Forge material at two different magnifications. This gives an impression of the homogeneity of the distribution, which in general is good (at least on a scale of up to a few tens of μm). The particulate in this material was sieved down to a few μm, and there are no particles larger than about 3 μm, which indeed was the target size for this processing route. There is also a significant proportion of finer particles. These probably originated partly from fines in the powder sample and partly from a certain amount of fracture of the larger particles during the manufacturing process. A further point to note here is that the material is apparently free of any porosity.

There is also interest in the matrix grain structure and the possibility of texture, which is most conveniently studied via EBSD images and associated pole figures. An example can be seen in **Figure 2**, which shows an x–z section from the Coarse-30-Forge material. There are indications here of partial recrystallization, probably with lateral growth inhibited (via Zener pinning) by very fine oxide particles that have become aligned in the vertical direction (normal to the forging direction). Such structures are quite common in MMC materials of this type,[12,13] with the oxide particles coming from the free surfaces of the original aluminum particles. The pole figure in Figure 2 indicates that some texture has developed during this process, although it is
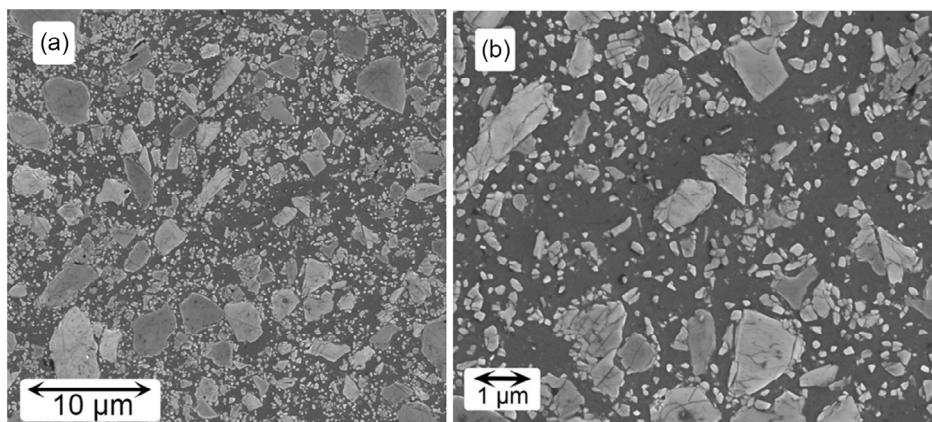

Figure 1. SEM micrographs showing typical microstructures in the x–y plane of the Coarse-30-Forge sample at a) low and b) high magnifications.
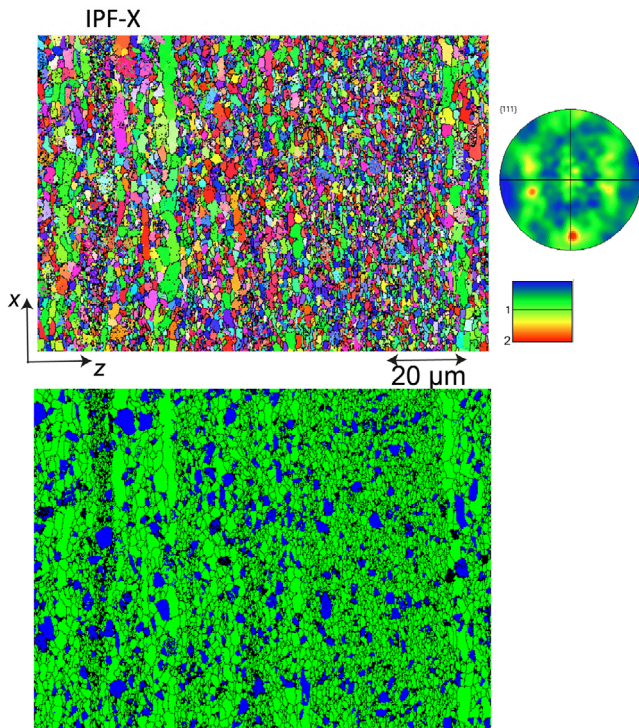
**ADVANCED
SCIENCE NEWS**

www.advancedsciencenews.com

**ADVANCED
ENGINEERING
MATERIALS**

www.aem-journal.com

Figure 2. EBSD images from an *x*–*z* plane of the Coarse-30-Forge sample, showing (top) that from the matrix, with a (111) pole figure, and (bottom) the distribution of the SiC particulate.

relatively weak. This is consistent with the recrystallization being quite limited. Partial recrystallization of this type could contribute to local inhomogeneity in the material, with the recrystallized grains being relatively soft. It may also be relevant in terms of anisotropy that could be exhibited by this material, although the distribution of particulate is also likely to influence this—see below. The other forged materials also exhibit similar features.

3.3. Optical Microscopy

Optical microscopy is helpful for study of the particle distribution on a relatively coarse scale. In the following micrographs, the

structures are shown (at two magnifications) for both in-plane (*x*–*y*) and transverse (*x*–*z*) sections. **Figure 3** relates to the HIPed material. As expected, there is no clear directionality on a macroscopic scale in this material. However, on the scale of an indent—typically of the order of several hundred microns in depth and perhaps a mm in width—there is in places a degree of alignment of the particulate into "stringers". The regions that appear light in these micrographs are depleted of particles, and these are indicative of such alignment in some locations. Such variations could have the effect of giving profiles—particularly pile-up heights—that vary in different directions, or even of introducing a difference between the profiles on the two halves of a single scan. The likelihood of this is difficult to assess from such micrographs, partly because the subsurface microstructure will also affect the behavior. It is also unclear whether pile-up heights are in fact very sensitive to the microstructure in the immediate vicinity of the pile-up or are also affected strongly by the nature of material in deeper and more central locations. Nevertheless, inhomogeneities of this type, on this scale, have the potential to create apparent anisotropies or anomalies. It might be expected that this would be more apparent with smaller ball radii, although this is likely to depend on the sensitivity of pile-up height to the microstructure of local or more remote regions.

The microstructures of the forged materials do appear to show some overall directionality—see **Figure 4** and **5**. This takes the form of alignment parallel to the *x*–*y* plane, which is apparent in the *x*–*z* sections. However, they also show inhomogeneities of a similar type to that apparent in Figure 3. This is clearer in the *x*-*y* sections.

The material with the coarser particulate (Coarse-30-Forge) also shows a similar type and degree of alignment (**Figure 6**). There is also some evidence of clustering (variations in local particle volume fraction), which can be seen more clearly than with the finer particulate. In fact, this occurs on scales ranging from a few tens of µm to a few hundreds of µm. Overall, however, the level of macroscopic homogeneity is good. It may be noted that this type of clustering is not necessarily clear in higher magnification (SEM) micrographs, such as those in Figure 1. It is potentially helpful to bear in mind the nature of these effects when considering various aspects of the PIP outcomes.
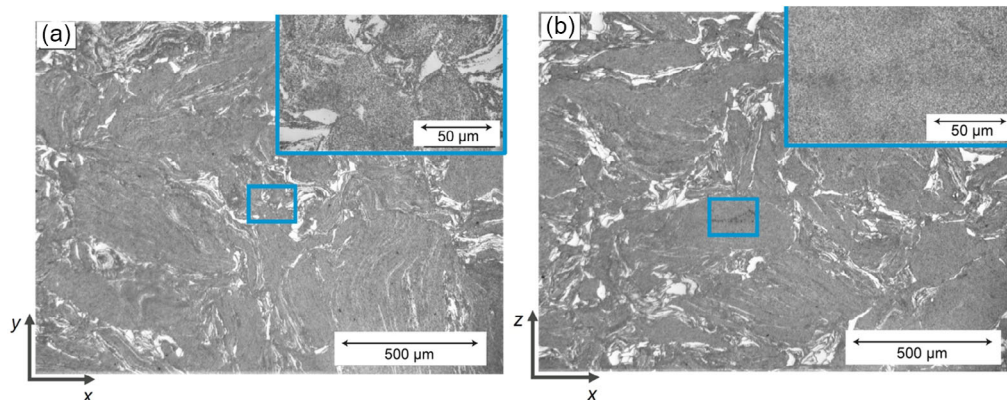

Figure 3. Optical micrographs showing typical microstructures of the Fine-20-HIP sample in: a) *x*–*y* and b) *x*–*z* planes.

ADVANCED
SCIENCE NEWS
www.advancedsciencenews.com

ADVANCED
ENGINEERING
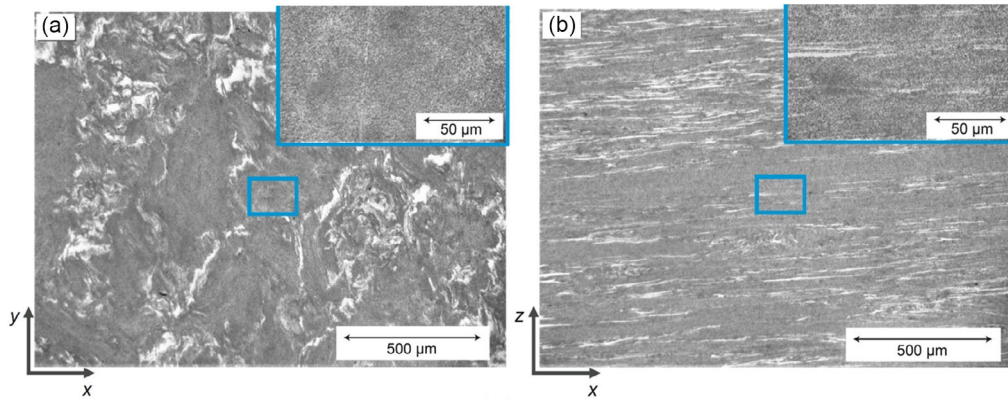MATERIALS
www.aem-journal.com

Figure 4. Optical micrographs showing typical microstructures of the Fine-20-Forge sample in: a) x–y and b) x–z planes.
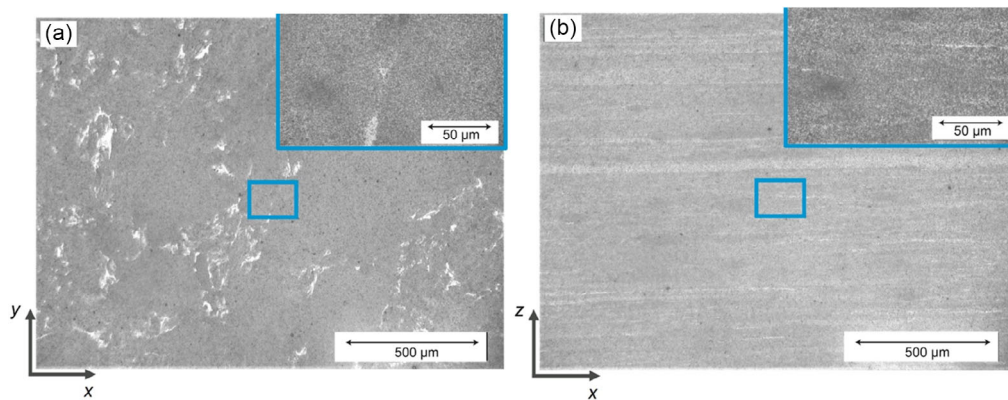

Figure 5. Optical micrographs showing typical microstructures of the Fine-30-Forge sample in: a) x–y and b) x–z planes.
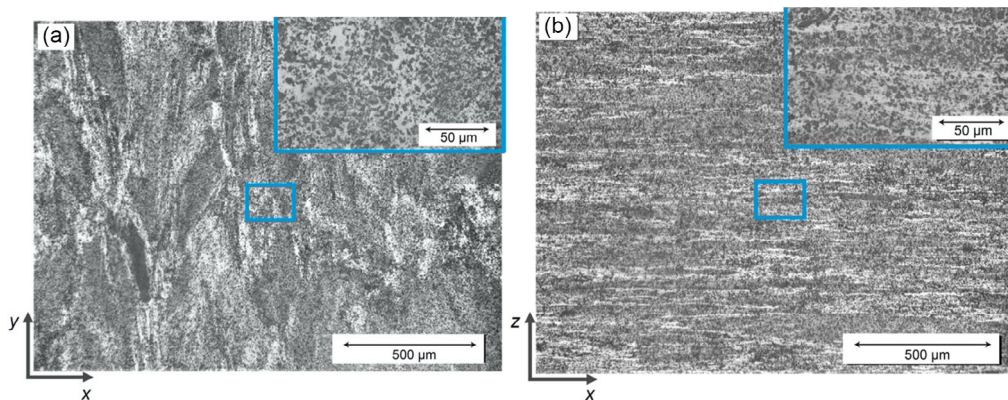

Figure 6. Optical micrographs showing typical microstructures of the Coarse-30-Forge sample in: a) x–y and b) x–z planes.

4. Mechanical Characteristics

4.1. Uniaxial Test Outcomes

The four experimental tensile (nominal) stress–strain curves are shown in **Figure 7**a, while the corresponding compressive curves are shown in Figure 7b. Compression testing has been carried out in both in-plane (x or y) and through-thickness (z) directions, while the tensile test samples were all loaded in an in-plane direction only. Certain features can be noted at this point. First, all curves have a noticeably transient shape during initial yielding. This has been reported previously and is probably a consequence of residual stresses in the matrix causing the yielding to take place progressively. This shape makes it particularly important to look at complete stress–strain curves, rather than trying to extract specific values for the yield stress.
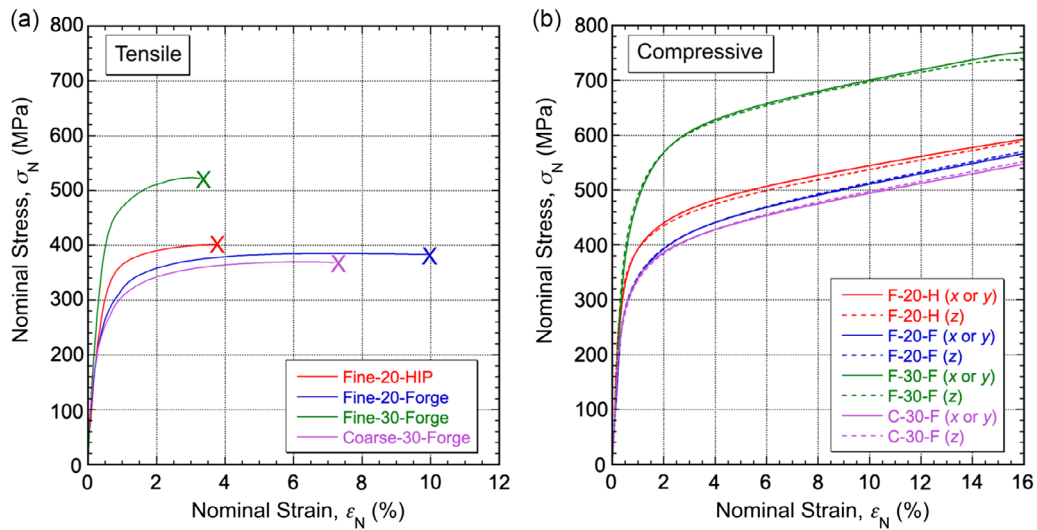
Figure 7. Typical plots of nominal stress against nominal strain for all 4 types of material, under a) tensile (*x* or *y*) and b) compressive (*x* or *y* and *z*) loading.

The differences between the four MMC types look plausible. Raising the particulate content (green v. blue curves) increases the hardness and reduces the ductility, as expected. Also, using finer particulate (green v. purple curves) has a similar effect. This suggests that the finer (0.7 μm) particles are causing some inhibition of dislocation mobility. Switching from forging to HIPing (red v. blue curves) appears to raise the hardness slightly and reduce the ductility. The ductility reduction could be due to lower homogeneity in the HIPed material.

There is good consistency between tensile and compressive curves. Of course, the shapes look different when presented as nominal plots, but the onset of yielding is occurring at similar stress levels in all four cases, with similarly transient behavior. To check for consistency at higher plastic strains, both must be converted to true stress–strain curves. **Figure 8** shows the outcome of this operation, with the conversions made using the standard analytical expressions. This can only be done up to the onset of necking for the tensile curves. For the compressive curves, this simple conversion takes no account of the effect of friction. Since this raises the experimental (nominal) curves to higher stress levels, typically by about 5–10%, the true stress in the compressive curves should be correspondingly reduced. When this is done, the agreement in Figure 8 between compressive and tensile plots is very good.

The other main point to be noted from the compressive curves in Figure 7b is that they indicate that, macroscopically, all of these materials are at least approximately isotropic. This is not unexpected, certainly for the HIPed material and possibly for the forged material as well. While the microstructures in Figure 4–6 suggest that some anisotropy might be expected, it is not surprising that this alignment of the particulate into "planes" of high particle content apparently does not lead to any strong effects overall.

4.2. PIP Indent Profiles

Among the first points to be checked during PIP testing is whether samples appear to exhibit inhomogeneity and/or
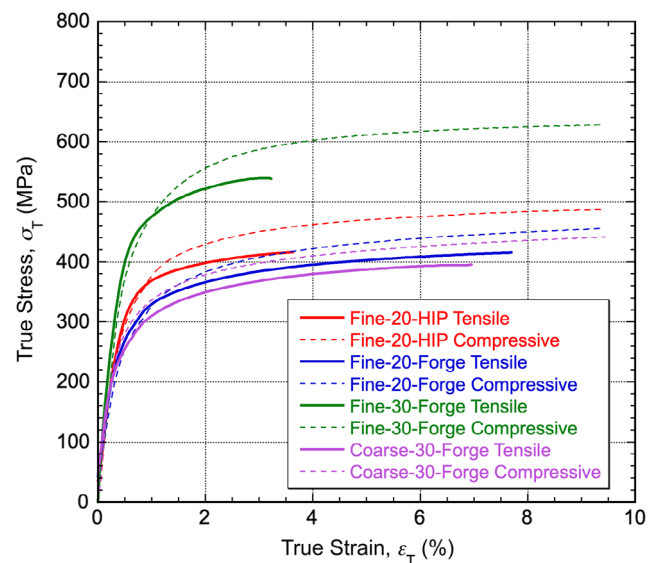

Figure 8. Comparison between true stress–strain curves derived from the two sets of experimental nominal plots (Figure 1): for compression, only those for the in-plane (*x* or *y*) tests are shown.

anisotropy. Inhomogeneity can be investigated by simply creating indents in a variety of locations (on a given plane, in a given sample) and monitoring any variations in the corresponding indent profiles. For these samples, it was found that there was little systematic change, although there were certainly some apparently fairly random variations. They can thus be taken to be macroscopically homogeneous, although apparently with some local variations in structure. This is broadly consistent with the microstructural evidence.

Anisotropy is conventionally detected during PIP testing in the form of a systematic lack of radial symmetry in the indent profiles—particularly the pile-up heights. Such variations were

**ADVANCED
SCIENCE NEWS**

www.advancedsciencenews.com

**ADVANCED
ENGINEERING
MATERIALS**

www.aem-journal.com

certainly detected in the current work, although they did not appear to be entirely systematic. Typical profile scans (obtained using stylus profilometry) from the HIP material, for both in-plane and transverse surfaces, are shown in **Figure 9**. These are not fully consistent with a general expectation of isotropy for the HIPed material, and with the compression test results

in Figure 7b, although some of them do show sufficient radial symmetry for a stress–strain curve to be inferred. These variations are apparently caused by local differences in particulate content and distribution of a type that is apparent in Figure 3.

Some systematic anisotropy was detected in the forged samples. Typical scans can be seen in **Figure 10**, which shows indent
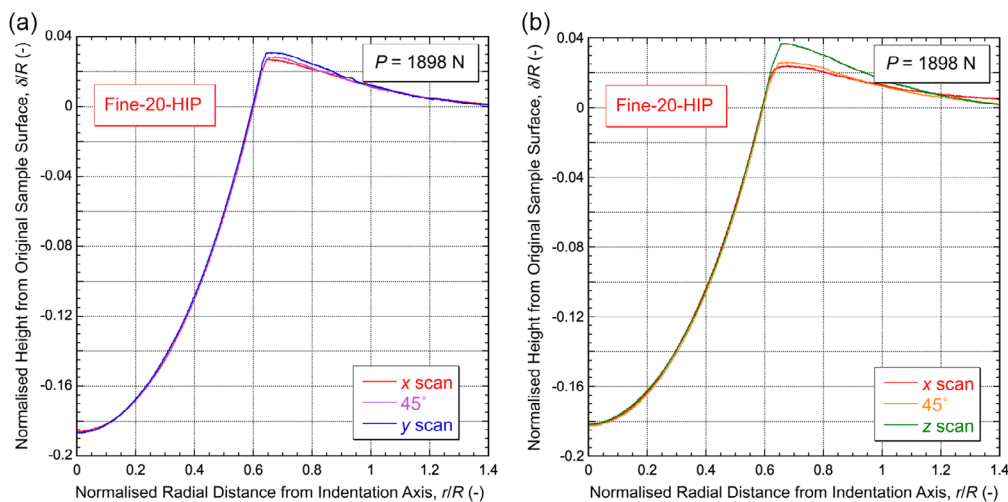

Figure 9. Typical measured PIP indent profile scans for HIPed samples on a) top (*x–y*) and b) transverse (*x–z*) planes, obtained using an indenter ball of 1 mm radius.
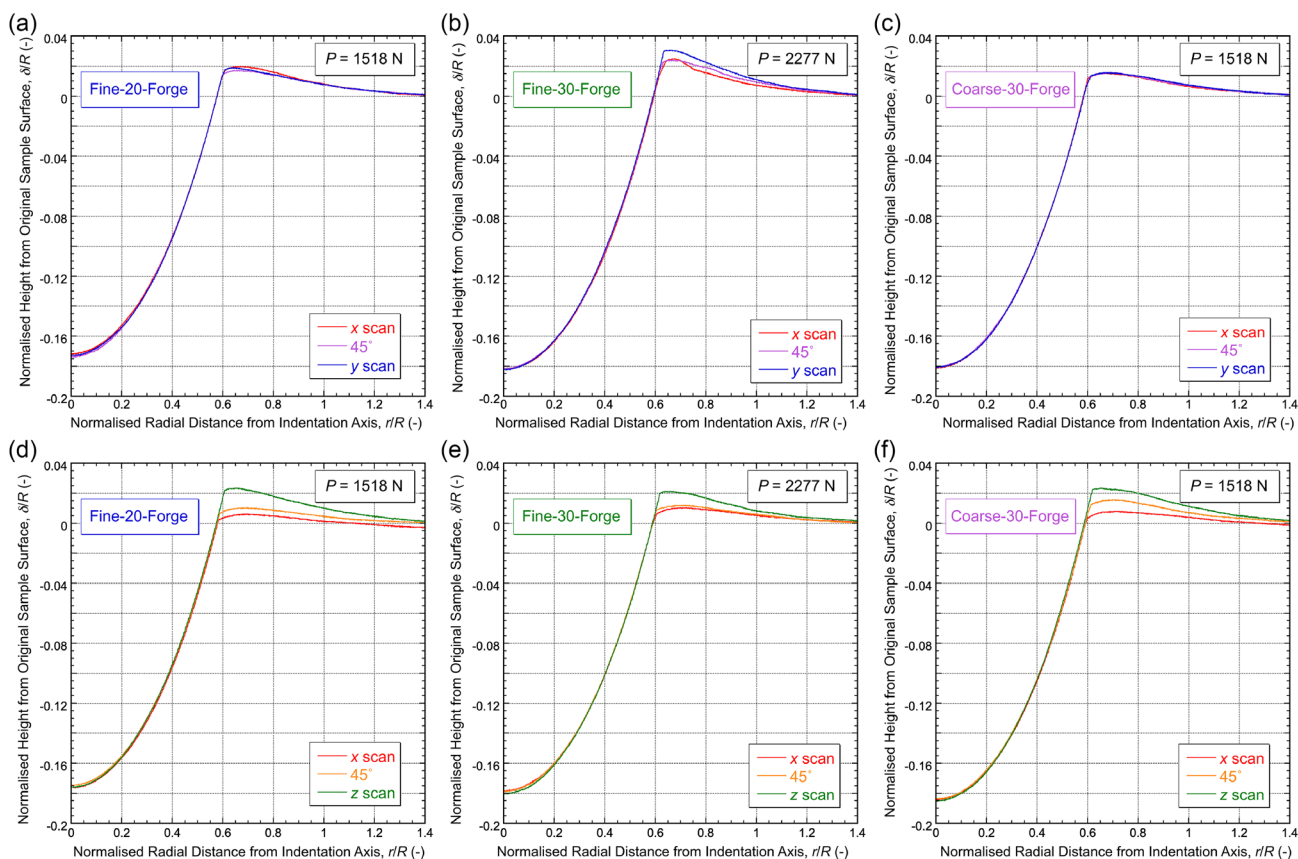

Figure 10. Typical measured PIP indent profile scans for forged samples on, a–c), top (*x–y*) planes and, d–f), transverse (*x–z*) planes.

**ADVANCED
SCIENCE NEWS**

www.advancedsciencenews.com

**ADVANCED
ENGINEERING
MATERIALS**

www.aem-journal.com

profiles in both types of plane, for all three of the forged materials. Many of those in the x–y plane do exhibit radial symmetry, indicating the expected isotropy, but there were again some cases where a degree of asymmetry was observed. In the x–z plane, the asymmetry appeared to be much more systematic, with the z direction being noticeably softer, suggesting that there is some overall anisotropy. These observations are broadly consistent with the local particulate distributions, as shown in Figure 4–6. The presence of "layers" with higher particulate content, oriented parallel to the x–y plane, will tend to make the in-plane directions a little harder than the through-thickness (z) direction, as observed.

For cases in which there is asymmetry in the radial profiles, the standard PIP procedure cannot be used to obtain stress–strain relationships (since it requires a single profile as the target outcome, with radial symmetry assumed in the associated FEM model). Indentation generates strains in all directions, so any stress–strain curve inferred from such a test will tend to be a direction-averaged one. Nevertheless, there were a number of indents that exhibited radial symmetry, at least to a good approximation, and these were used to obtain stress–strain curves.

4.3. Optical Profilometry and Effects of Ball Radius

To explore the nature of these apparently rather random variations in the details of profile shape, several indents were made in the Fine-20-HIP material, using balls with radii of 0.5, 1.0, 1.5, and 2.0 mm. The outcome can be seen in **Figure 11**, in which pile-up height is plotted as a function of scan angle, normalized by indent depth, for 2 indents with each ball radius.

The picture here is not a simple one. While there appears to be a slight tendency for the variations to be smaller in amplitude with the larger balls, this trend is certainly not consistent or marked. Furthermore, the fluctuations appear to be completely

random, with it being relatively rare for the pile-up height to be the same at both ends of a single scan (separated by 180° in scan angle). These variations are evidently not caused by consistent anisotropy in the samples and in fact it is clear that they are due to inhomogeneities in microstructure. Moreover, similar plots were obtained in the x–z plane (and indeed, for the HIPed material, it is not possible to identify different directions in terms of the processing conditions).

The diameters of these indents were about 0.7, 1.4, 2.1, and 2.8 mm. The regions being deformed are increasing in volume as the ball radius is raised, reaching levels that would certainly be expected to smooth out the kind of microstructural inhomogeneities that are apparent in Figure 2 and 3. It follows that the pile-up heights must be quite sensitive to the microstructure in their immediate vicinity. Even for the largest ball used here, that region may be just a few hundreds of microns in "width," or possibly even less. The depth of the region that most strongly affects the pile-up height is probably similar.

However, the data for the forged samples are more consistent and do indicate the presence of overall anisotropy. A plot of the same type as Figure 11, covering all the materials, is shown in **Figure 12**. For indents in the x–y plane (solid lines), the picture for the forged samples is similar to that for the HIPed sample— i.e., there are some fairly random variations, although they are less pronounced than in the HIPed material. In the x–z plane (dotted lines), in contrast, a more consistent picture emerges for the forged materials, with these plots approximating to the expected shape—i.e., there is a well-defined direction in which the pile-up height is appreciably higher (and virtually all scan directions are symmetric about the central axis, so that heights are similar for any two directions that are 180° apart). The material is "softer" in this direction, which is the z (through-thickness) direction. The "hardest" direction is expected to be normal to this. This is consistent with the microstructures seen in Figure 4–6 and the complete profiles in Figure 10. This
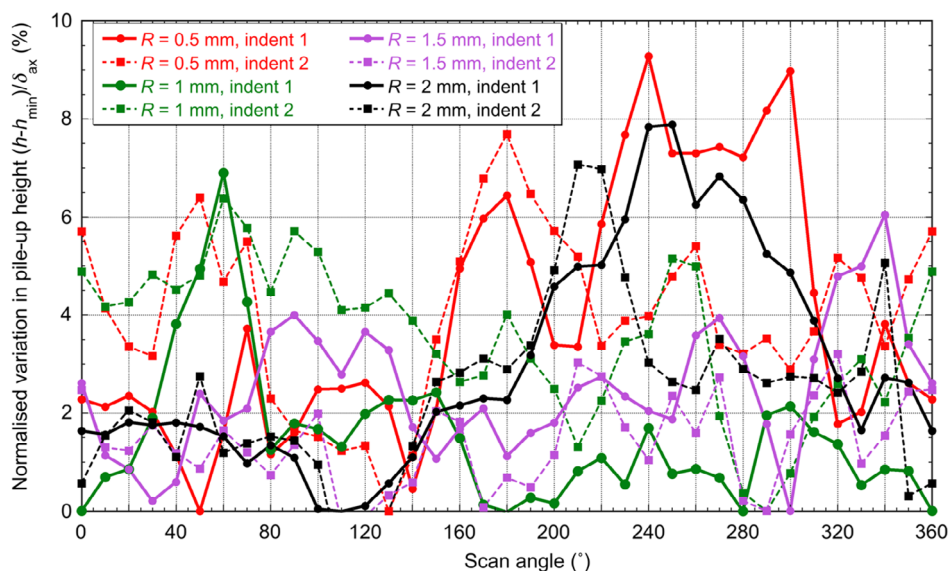

Figure 11. Representative variations in pile-up height, as a function of scan angle, for indents in the x–y plane of Fine-20-HIP, for 4 ball radii. Optical profilometry was used for this work.
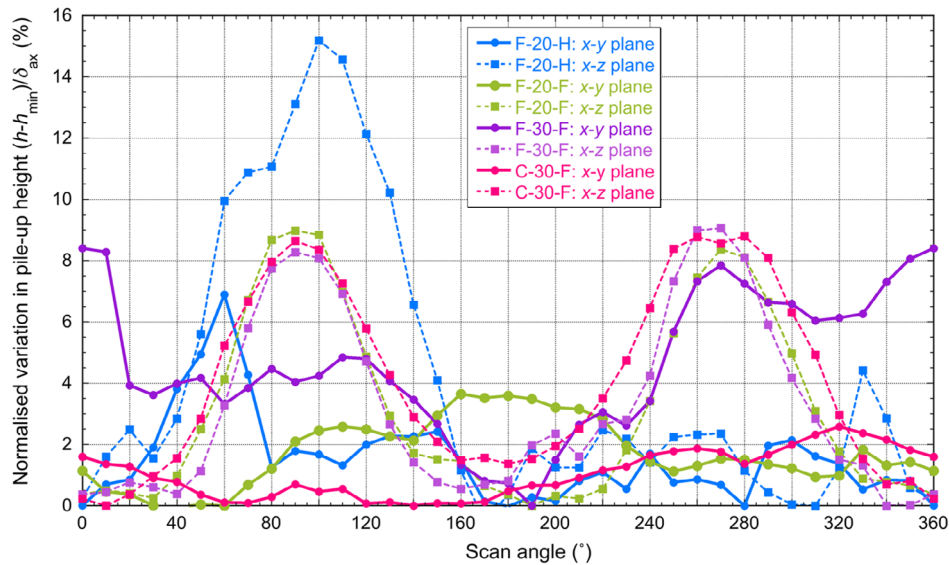
Figure 12. Typical measured variations in pile-up height, as a function of scan angle, for indents in all of the samples, into both types of plane, created using an indenter ball of radius 1 mm. Values are normalized by the indent depth.

demonstrates the high sensitivity of PIP for detecting such anisotropy, which is not picked up by the uniaxial compression testing.

4.4. Uniaxial and Profilometry-Based Indentation Plastometry-Inferred Stress–Strain Curves

The standard PIP procedure involves converting a (radially symmetric) indent profile to a (best-fit) true stress—true plastic strain curve (in the form of a V_{oce} constitutive relationship, with a given set of parameter values). This has been done in the present work for profiles that did exhibit such symmetry. Subsequent checking with the optical profilometer confirmed that they were at least approximately symmetric radially. It should perhaps be noted that, while the scans in Figure 11 show that quite

significant pile-up height variations (of the order of up to a few tens of microns) may be present, they can be smoothed out and the differences between the averaged profile and the "outliers" will in many cases be quite small.

The resultant true stress–strain curve can be converted to a nominal one for uniaxial loading (tensile or compressive). This is most easily done using the well-known analytical relationships, although the points made above concerning these conversions should be noted. Both the post-necking regime in tensile testing and the effect of friction in compression can be obtained from the true stress–strain curve via FEM modeling, although this must be done for the specific sample dimensions (and friction conditions) of the test.

Since the experimental tension and compression curves are in good agreement, it is logical to just compare the PIP-derived curves with one of these sets. This has been done in **Figure 13**
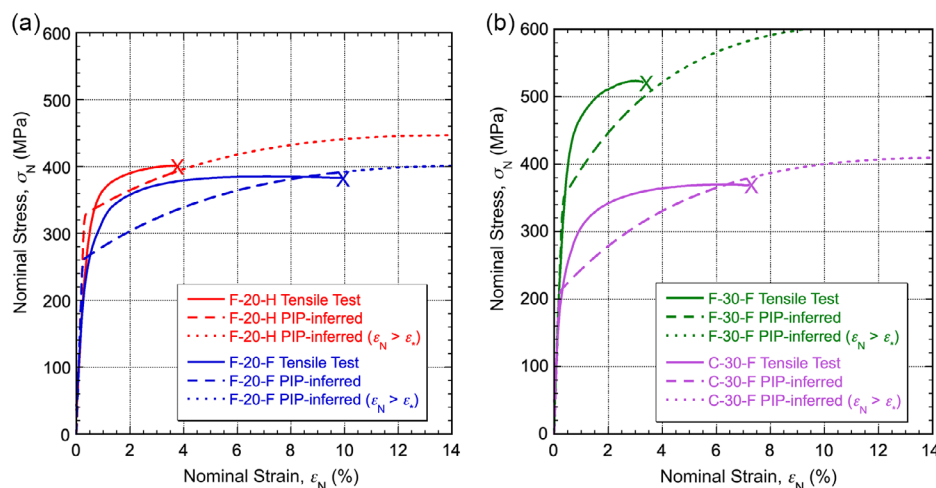

Figure 13. Comparison between (nominal) tensile stress–strain curves from uniaxial testing and PIP testing for: a) 20% particulate MMCs and b) 30% particulate MMCs.

for the tensile (nominal) plots. A couple of points should be noted. First, two of these materials—the Fine-20-HIP (red) and the Fine-30-Forge (green)—fractured before necking. This could be regarded as "premature" fracture, which cannot be picked up by PIP testing. Second, the PIP procedure is relatively insensitive to a transient nature in the onset of yielding, which cannot be captured via a set of V_{oce} parameter values. This is evident in the PIP-derived curves. Nevertheless, they do capture well both the yield stresses and the general nature of the work hardening (and give reliable UTS values, particularly if the curves are curtailed at the fracture strain for the materials exhibiting "premature" fracture). Among other points, this agreement suggests that "crowding" (a proposed tendency for the volume fraction of particulate to increase in certain locations as a result of plastic straining—changing the stress–strain relationship)—is not a significant effect. In any event, PIP clearly has the potential for study of local inhomogeneities and anisotropy, and this is likely to be of particular interest for testing of particulate MMCs.

5. Conclusions

This study concerns the response of Al-based particulate MMCs to profilometry-based indentation plastometry (PIP) testing. Comparisons are made between outcomes from this type of test and from conventional uniaxial (tensile and compressive) testing. Four different types of MMC, with variations in particle size and volume fraction, have been examined. The following conclusions can be drawn: 1) In general, good agreement is observed between the stress–strain curves obtained via PIP testing and via conventional uniaxial testing. This indicates that the PIP testing involves deformation of a volume that is large enough to be representative of the bulk. This is potentially a concern for materials such as MMCs, since a representative volume clearly needs to incorporate a relatively large number of reinforcement particles; 2) Even with relatively large ball radii, significant (random) variations have been observed in pile-up height, as a function of scan angle. Such variations would normally be indicative of anisotropy. However, with the MMC material produced by HIPing, no such anisotropy is expected and indeed uniaxial testing confirmed that it is isotropic. The variations are attributed to local differences in microstructure – particularly in particle volume fraction – on a fairly coarse scale ($\approx$hundreds of microns). PIP thus constitutes a sensitive methodology for detecting such (relatively coarse) inhomogeneities; 3) With the forged materials, in contrast, the microstructure is such that some anisotropy is expected. The particles have become somewhat concentrated into planes lying normal to the forging direction, which is expected to lead to the through-thickness direction being slightly softer than the in-plane directions. Measured variations in pile-up heights for directions within transverse planes are fully consistent with this. The sensitivity of the PIP procedure to detection of such effects is high, since this anisotropy was not strong enough to be detected by conventional uniaxial testing; 4) These materials exhibit quite strongly transient yielding. This cannot be picked up by PIP testing, so the initial parts of the curves look slightly different for the two types of test. Nevertheless, the values obtained for the yield stress are in good agreement for all of the materials tested; and

5) A further point to note about these materials is that, while they exhibit good toughness, there is a tendency for the strain to failure (ductility) values to be relatively low ($\approx$4–10%). In particular, they may fracture before the onset of necking. If this happens, then a (relatively small) discrepancy may arise between the UTS value obtained by PIP testing (which corresponds to the onset of necking) and that from a tensile test.

Conflict of Interest

The authors declare no conflict of interest.

Data Availability Statement

The data that support the findings of this study are available from the corresponding author upon reasonable request.

[1] M. Taya, K. E. Lulay, D. J. Lloyd, *Acta Metall. Mater.* **1991**, *39*, 73.

[2] S. F. Corbin, D. S. Wilkinson, *Acta Metall. Mater* **1994**, *42*, 1329.

[3] J. Llorca, C. Gonzalez, *J. Mech. Phys. Sol.* **1998**, *46*, 1.

[4] Y. L. Shen, N. Chawla, *Mater. Sci. Eng., A* **2001**, *297*, 44.

[5] H. Berns, *Wear* **2003**, *254*, 47.

[6] K. M. Shorowordi, A. S. M. Haseeb, J. P. Celis, *Wear* **2004**, *256*, 1176.

[7] A. A. Mazen, M. M. Emara, *J. Mater. Eng. Perform.* **2004**, *13*, 39.

[8] Z. Y. Yang, J. Z. Fan, Y. Q. Liu, J. H. Nie, Z. Y. Yang, Y. L. Kang, *Materials* **2021**, *14*, 675.

[9] A. M. Sankhla, K. M. Patel, M. A. Makhesana, K. Giasin, D. Y. Pimenov, S. Wojciechowski, N. Khanna, *J. Mat. Res. Technol.* **2022**, *18*, 282.

[10] P. B. Prangnell, S. J. Barnes, S. M. Roberts, P. J. Withers, *Key Eng. Mater.* **1997**, *127–131*, 937.

[11] A. M. Murphy, S. J. Howard, T. W. Clyne, *Mater. Sci. Technol.* **1998**, *14*, 959.

[12] R. A. Shahani, T. W. Clyne, *Mater. Sci. Eng.* **1991**, *135*, 281.

[13] A. F. Whitehouse, R. A. Shahani, T. W. Clyne, *J. Microsc.* **1995**, *178*, 208.

[14] C. Davis, J. Allison, *Metall. Mater. Trans. A* **1993**, *24*, 2487.

[15] G. Meijer, F. Ellyin, Z. Xia, *Composites, Part B* **2000**, *31*, 29.

[16] H. T. Liu, L. Z. Sun, *Int. J. Solids Struct* **2004**, *41*, 2189.

[17] C. S. Wong, A. Pramanik, A. K. Basak, *Mater. Sci. Technol.* **2018**, *34*, 1388.

[18] R. R. Balokhonov, A. S. Kulkov, A. V. Zemlyanov, V. A. Romanova, E. P. Evtushenko, D. D. Gatiyatullina, S. N. Kulkov, *Phys. Mesomech.* **2021**, *24*, 503.

[19] T. W. Clyne, J. E. Campbell, M. Burley, J. Dean, *Adv. Eng. Mater.* **2021**, *23*, 2100437.

[20] J. E. Campbell, H. Zhang, M. Burley, M. Gee, A. T. Fry, J. Dean, T. W. Clyne, *Adv. Eng. Mater.* **2021**, *23*, 2001496.

[21] T. W. Clyne, J. E. Campbell, *Testing of the Plastic Deformation of Metals*, Cambridge University Press, Cambridge, UK **2021**, https://doi.org/10.1017/9781108943369.

[22] W. Gu, J. E. Campbell, Y. T. Tang, H. Safaie, R. Johnston, Y. Gu, C. Pleydell-Pearce, M. Burley, J. Dean, T. W. Clyne, *Adv. Eng. Mater.* **2022**, *24*, 2101645.

[23] J. W. Leggoe, X. Z. Hu, M. V. Swain, M. B. Bush, *Scr. Metall. Mater.* **1994**, *31*, 577.

[24] K. M. Mussert, W. P. Vellinga, A. Bakker, S. Van Der Zwaag, *J. Mater. Sci. Technol.* **2002**, *37*, 789.

[25] Y. L. Shen, J. J. Williams, G. Piotrowski, N. Chawla, Y. L. Guo, *Acta Mater.* **2001**, *49*, 3219.

[26] R. Ekici, M. K. Apalak, M. Yildirim, F. Nair, *Mater. Des.* **2010**, *31*, 2818.

[27] A. S. Shedbale, I. V. Singh, B. K. Mishra, *Mech. Adv. Mater. Struct.* **2021**, *29*, 4427.

[28] R. Pereyra, Y. L. Shen, *Int. J. Damage Mech.* **2005**, *14*, 71.